Optical Feedback Tweezers

Avinash Kumar and John Bechhofer

Department of Physics, Simon Fraser University, Burnaby, BC, Canada

ABSTRACT

Feedback traps can manipulate particles arbitrarily. In a feedback trap, a position detector detects the particle's position, a computer calculates the necessary force to be applied based on the position in the "virtual potential", and is applied periodically on the particle. Previous feedback traps have used electrokinetic or hydrodynamic forces to manipulate particles. Here, we use an optical trap as a source of force in feedback trap to impose arbitrary potentials. We create feedback forces on optically trapped particles by moving the trap position rapidly in response to observed fluctuations with the help of an acousto-optic deflector (AOD). Preliminary experiments show that we can confine a 1.5 μm silica bead in a "virtual potential" that is 35–40 times stiffer than the underlying optical trap, whose laser power is kept constant. We also present preliminary results for a virtual double-well potential. We show that we can independently control the well separation and barrier height of these virtual double-well potentials, that is impossible to do with time-sharing of optical tweezers.

Keywords: Optical tweezers, feedback trap, virtual potential

1. INTRODUCTION

After their development by Ashkin et al.,[1] optical tweezers have been widely used for exerting forces on small mesoscopic particles in different areas of science. It is one of the most widely used non-invasive techniques for understanding dynamics of biological motor proteins,[2] DNA unfolding,[3,4] colloidal particles,[5] etc. Feedback controlled optical tweezers have enabled the biophysics community to explore the colloidal dynamics with higher resolution and bandwidth. In a feedback trap, a control force is calculated based on particle's position in a desired "virtual potential" and is applied to the particle. Ashkin et. al. first used optical tweezers to apply feedback forces on an optically levitated particle in air.[6] Later on, other techniques were used to apply feedback forces such as magnetic forces,[7] microfluidic flow forces,[8] opto–thermoelectric forces,[9,10] and electrokinetic forces.[11]

In this paper, we present first results of attempts to create arbitrary virtual potentials with optical feedback forces. We show that, for a virtual harmonic potential and a double-well potential, the potential reconstructed from Boltzmann distribution is consistent with the imposed form. The feedback-trap technique to create arbitrary potentials by applying a desired control-force to counteract random fluctuation of a diffusing particle was

developed by Cohen and Moerner.[11,12] Here, instead of counteracting the Brownian motion of the freely diffusing particle by using electrokinetic forces, we use optical tweezers to exert the desired forces on the particle. A particle in an optical trap with stiffness k experiences a linear restoring force, $F = -kx$, for small displacement, x from the trap centre. The trap can be modelled as a damped spring-mass system. Similarly, if the trap centre is shifted by a small amount, the "Hookean-like" force, $F = -kx$ will still exist. We use this technique to counter the Brownian fluctuations of the particle. These feedback forces are different from real trap forces. In a real trap, the restoring force changes continuously with the particle's position. On the contrary, in a closed feedback loop, the force is updated only once per cycle time, Δt. Thus, the trap formed by shifting the trap centre to clamp a particle is "virtual" in nature. As long as $\alpha \ll 1$, the virtual potential approximates the real trap potential.[13]

Previously, several groups have explored adding feedback to optical tweezers to increase the trap stiffness. Simmons et al. used a two-dimensional analog feedback control with two orthogonal acousto-optic modulators and achieved a 400-fold gain in the stiffness of the trap.[14] Ranaweera et al.[15] and Wallin et al.[16] used proportional control to increase the trap stiffness by a factor of 29 and 10, respectively. In our experiment, a linear control algorithm can create a virtual trap 35–40 times stiffer than the underlying potential.

Virtual potentials have been used to study fundamental questions in statistical physics. Jun et al. used feedback trap to test Landauer's principle for erasure of information[17] at higher precision than earlier work by Bérut et al., which used a time–dependent, multiplexed, double–well potential.[18]

In the present work, we create arbitrary time-dependent virtual potentials with optical tweezers. We show that we can impose a "virtual potential" using forces from an optical tweezer and have it agree with the potential reconstructed from the Boltzmann distribution to $\approx 5\%$. A very accurate calibration of parameters is necessary to apply the right amount of force on the particle. We first tested our feedback trap with a simple example of harmonic potential. We also created a static double-well potential. With our feedback trap, we can create a family of curves for a double-well potential and independently change the barrier height and well separation which is impossible with an ordinary optical tweezer.

2. VIRTUAL FEEDBACK TRAP USING OPTICAL TWEEZERS

Our feedback scheme is based on the work of Gavrilov et al.[19] A quadrant photodiode (QPD) is used to estimate the position of the particle (Fig. 1a). From the observed position, the required force based on a chosen potential is calculated (Fig. 1b). The force is generated by the displacement of the trap centre (Fig. 1c). A small displacement relative to the trap centre will create a linear restoring force on the particle. If we repeat these steps in a closed loop, we can confine the particle in a virtual potential. We can consider these forces as a discrete approximation

of the real physical potential. The cycle time for our experiment is 6 μs. In the absence of feedback, the trap centre tracks the particle, which diffuses randomly.

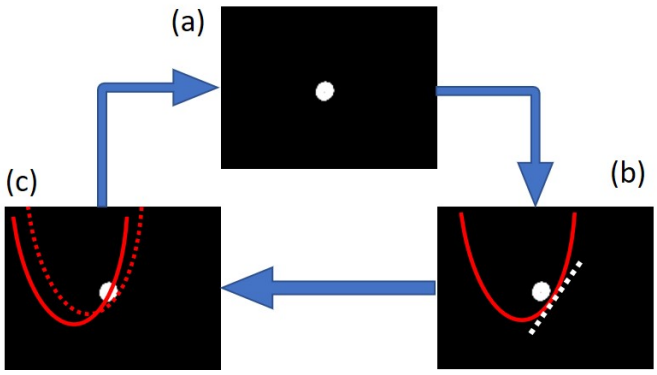

Figure 1. One cycle of a feedback trap: (a) Estimate the particle's coordinates, (x, y); (b) calculate force based on the chosen potential; and (c) shift the trap centre to apply force to the particle.

3. FEEDBACK DYNAMICS IN OPTICAL TWEEZERS

In a real potential, the force exerted on the particle is instantaneous and continuously changes with particle's position. It is proportional to the displacement of the particle from the trap centre. The discrete dynamics of a trapped particle in a real potential can be written as

$$x_{n+1} = x_n - \frac{\Delta t}{\gamma} k x_n + \zeta_n, \tag{3.1}$$

where $x_n(t_n)$ is the true position of the particle at time t_n, Δt is the sampling frequency, k is the stiffness of the optical trap, γ is the viscosity of the trapping medium, and ζ is the thermal fluctuation (white noise) where $\langle\zeta_n\rangle$=0, and $\langle\zeta_n\zeta_{n-1}\rangle = 2D\Delta t\delta_{n,n-1}$.[20] The diffusion constant can be calculated by $D = k_{\rm B}T/\gamma$, where $k_{\rm B}$ is Boltzmann constant and T is the temperature. For feedback traps, there is a time delay between the acquisition of particle's position and the application of the required force. Thus, we should notice the difference between the real position, $x_n(t_n)$ and the observed position of the particle, $\overline{x}_n(t_n)$. In our experiment, the time delay set to $t_{\rm d} = 5$ μs, which is also equal to the sampling time of the particle's position. The equation of motion for a particle in a virtual potential then becomes

$$x_{n+1} = x_n - \alpha(x_n - x_n^t) + \zeta_n, \tag{3.2a}$$

$$x_{n+1}^t = G(\overline{x}_{n-1} - x_{\rm set}) + x_n^t(1 - e^{(t-t_{\rm d})/t_{\rm r}}) \tag{3.2b}$$

where α is the dimensionless feedback gain given by $\alpha = \Delta t/t_{\rm r}$, with $t_{\rm r} = \gamma/k$ the relaxation time of the imposed harmonic potential and t_r is the rise time of the AOD control signal. The time delay $t_{\rm d}$ due to AOD is 10 μs.

The feedback gain α is similar to the spring constant, k in Hooke's law, $F(t) = -kx_n$. The force in a real trap changes continuously with position, whereas the force F = αx in a virtual potential is constant over the interval Δt. For $\alpha \ll 1$, the virtual potential is a very good approximation of the real force but the deviation from the real force increases for larger α.[13] The trap is shifted only once per cycle, and it remains clamped to the same position until it gets a new command in the next cycle.

4. EXPERIMENTAL SETUP

4.1 Trapping and detection system

Figure 2 shows the schematic of our optical tweezers setup with feedback mechanism. Our optical tweezers setup is built on a vibration isolation table (Melles Griot) that supports a custom-built microscope. An s-polarized 532 nm laser (Nd:YAG, Coherent Genesis MX STM-series, 1 Watt) is used for trapping. The laser passes through a Faraday isolator (LINOS FI-530-2SV, isolation >30 dB) which prevents back reflections from entering into the laser cavity. The output from the isolator goes through a spatial filter (SF), which produces a smooth Gaussian beam by blocking any aberrations present in the laser beam. The clean laser beam passes through a non-polarizing beam splitter cube that separates the detection and trapping laser. The same laser is used for both trapping and detection of the Brownian fluctuations. In situations where the trap position changes dynamically, we cannot use the trapping laser to also measure the particle's position. Thus, we pick off $\approx 10\%$ of the laser light using a beam splitter cube for detection of the trapped particle.

Both lasers pass independently through orthogonal XY-Acousto-Optic Deflectors. Each acousto-optic deflector can be used to modulate the intensity of the input light as well as to steer the angle of the beam. Orthogonally oriented AODs control the laser beam direction in two dimensions. There are other ways, reported in litrature, to steer the trap that uses spatial light modulators (SLM),[21] acousto-optic deflectors (AODs),[22,23] electro-optic deflectors (EODs),[24] piezo-mirrors[25] have been extensively used to apply feedback forces. SLMs and piezo-mirrors are limited in application due to lower bandwidth (100–200 Hz) whereas AODs and EODs are the best choices for closed-loop feedback operation because of high bandwidth ($\approx$ 1 MHz). The output of the trapping laser after the AOD-T is expanded by a factor of two to overfill the back aperture of the trapping objective. After the beam expansion, a relay system (1:1) of lenses is used to place the AODs at the back focal plane of the trapping objective to create pure translation of the trap in the trapping plane.

We use two identical water immersion high numerical aperture objectives (Olympus 60X, UPlanSApo, NA = 1.20 W) for trapping and detection. Water–immersion objectives provide a longer working depth without distorting the laser wavefront. The trapping objective is placed on a XY-piezo stage (Mad City Labs, H100) to provide a precise movement of trap inside the sample chamber. The trapping objective also serves as the detection

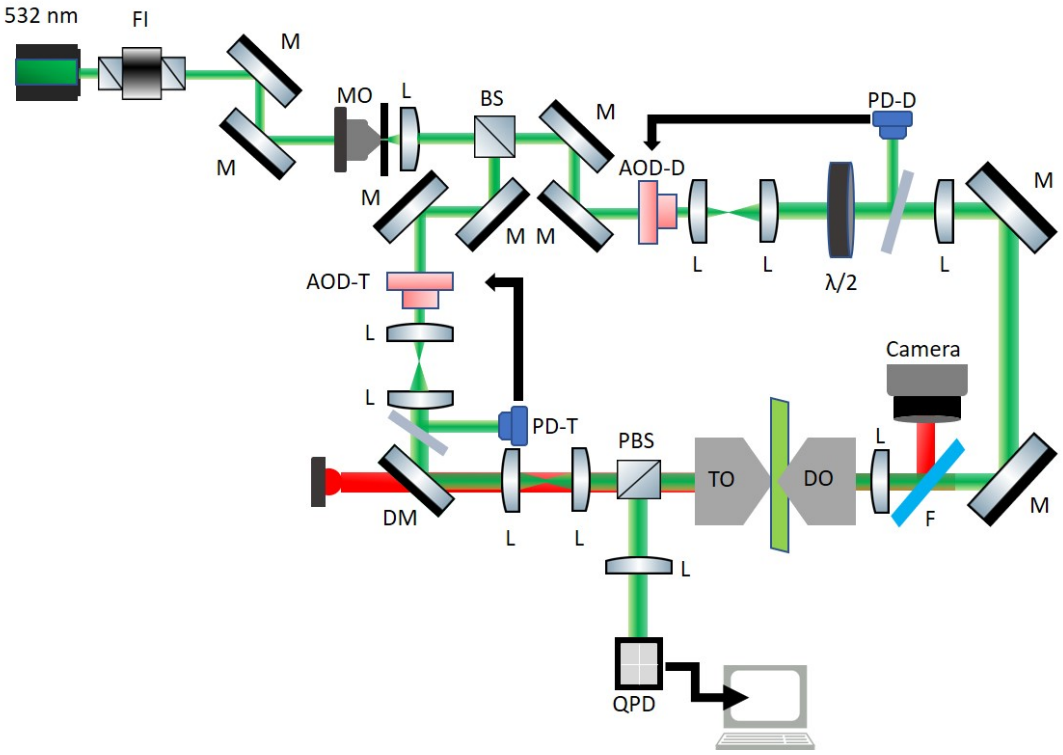

Figure 2. Schematic diagram of the setup for feedback trap. FI = Faraday Isolator, M = Mirror, MO = Microscope Objective, BS = Beam Splitter (non-polarizing), PD = Photodiode, AOD = Acousto-Optic Deflector, L = Lens, TO = Trapping Objective, DO = Detection Objective, PBS = Polarizing Beam Splitter, $\lambda/2$ = Half-Wave Plate, F = Short-Pass Filter, QPD = Quadrant Photodiode, DM = Dichroic Mirror.

objective in our experiment. The polarization of the detection beam is rotated by 90 degrees with a half–wave plate (Thorlabs, WPMQ05M-532) to avoid any interference between the trapping laser and the detection laser. We use this property to separate the detection laser from the trapping laser with a polarizing beam splitter cube.

A 660 nm LED (Thorlabs, M660L4) is used to illuminate the sample chamber. The illumination light is separated from the trapping laser using a shortpass filter before it enters the camera. The forward scattered light from the trapped particle is collected by the detection objective. We use a quadrant photodiode (QPD, First Sensor, QP50-6-18u-SD2) to detect the fluctuations of the particle. The photodiode is placed at a plane conjugate to the back focal plane of the detection objective. Two feedback loops independently regulate the AOD-T and AOD-D, to compensate for any fluctuation in the total laser power. The photodiodes, PD–T and PD–D monitor the power fluctuations in the outputs of the AODs.

4.2 Data Acquisition

A LabVIEW–based FPGA (Field–Programmable Gate Array) data acquisition system (NI 7855R) collects the voltage signals from the quadrant photodiode to send the control signals to the AODs. The FPGA card can run the control protocol in real time with deterministic time steps of 5 μs. Unlike standard computer processors, FPGA cards are not limited by the speed of the host computer. They can also run different processes in parallel without competing for resources. Each task is assigned to a dedicated section of the reprogrammable chip, which can function independently without influencing other logic blocks. We use the LabVIEW cloud to compile the FPGA code. The compilation process takes 10–15 min.

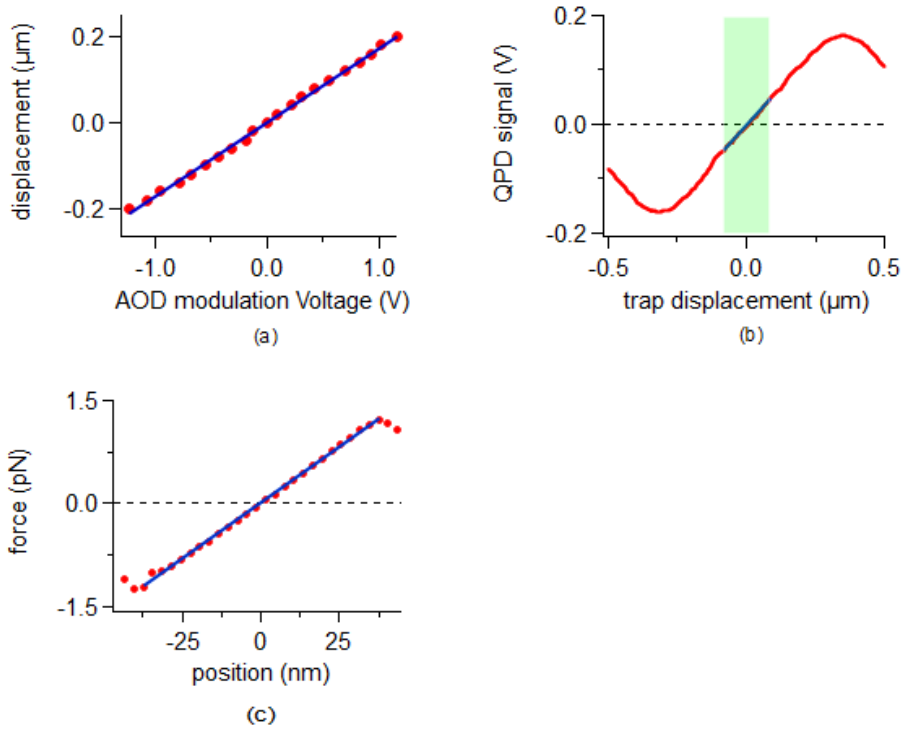

Figure 3. (a) The modulation voltage of the AOD is varied from -1.2 V to $+1.2$ V (~ 3 μm) to calibrate AOD. The plot shows a linear mapping between AOD modulation voltage and trap displacement. (b) QPD calibration plot shows the non-linear relation between the trap displacement and the QPD response. Although the AOD is linear over a range of ≈ 3 μm, the linear region of the QPD response is limited to 250 nm only.(c) Force calibration curve for a trapped particle. The force is linear over $\pm$ 45 nm form the trap centre.

4.3 Calibration

A three-step calibration process is used to map the voltage signals measured from QPD (V) to real units (μm). Since we are using two high NA microscope objectives for trapping and detection, the separation between them

is so small that we cannot use a normal micrometer scale to calibrate the camera. Instead, we used a silica bead of known size to calibrate the image. Using a silica bead of diameter 1.49 μm, we found that the average size of one pixel is 78 ± 4 nm. Next, we calibrate the trap displacement produced in the trapping plane because of the change in the modulation voltage in the AOD. Fig. 3a shows the response of the AOD for the change of the modulation voltage. We explored either sides of the trap centre by varying the modulation voltage from -1.2 to $+1.2$ V and the trap displacement in real units (μm) was measured from the displacement of the image on the camera. This is a one-time calibration process for the AOD, provided there is no change in the optics of the experiment.

Once we calibrate the camera and AOD, we should calibrate the response of QPD against the AOD modulation voltage. Fig. 3b shows a typical response of the QPD as a function of trap displacement. The response of the QPD is linear over a very small region ($\approx$ 250 nm) around the trap centre. Although the AOD is fairly linear over a bigger range, the small linear response of QPD acts as a bottleneck for linear control systems. A nonlinear calibration is required for larger trap displacements. QPD calibration is very sensitive to optical alignment. This calibration is done every time before taking data. Fig. 3c shows the force calibration curve for a trapped particle without any feedback. The force applied on the particle in a harmonic trap is linear within $\approx$2% over 45 nm on either side from the trap centre. Thus, a linear calibration for QPD–response and the force–calibration curve is sufficient for double–well experiment provided we choose a small well separation ($<$100 nm).

5. RESULTS

5.1 Virtual harmonic potential

The ability to create a harmonic potential is a basic function of feedback traps. We can change the value of feedback gain, α, to create traps with arbitrary stiffness. For small value of α, the variance of particle's fluctuation follows equipartition theorem. For higher values of α, the particle starts to oscillate due to overcorrection of fluctuations and is seen as the emergence of resonance peak in the power spectrum. The optimal value of feedback gain is where the variance is minimum. The frequency at which the resonance peak arises is dependent on the feedback time delay. The smaller the feedback delay, the greater is the maximum stiffness of the trap. In Fig. 4, we show the power spectra for different values of feedback gains. Zero feedback gain indicates the real harmonic trap without any feedback. We see that the feedback forces can create 35-40 times stiffer harmonic traps than the actual optical trap ($\alpha = 0$).

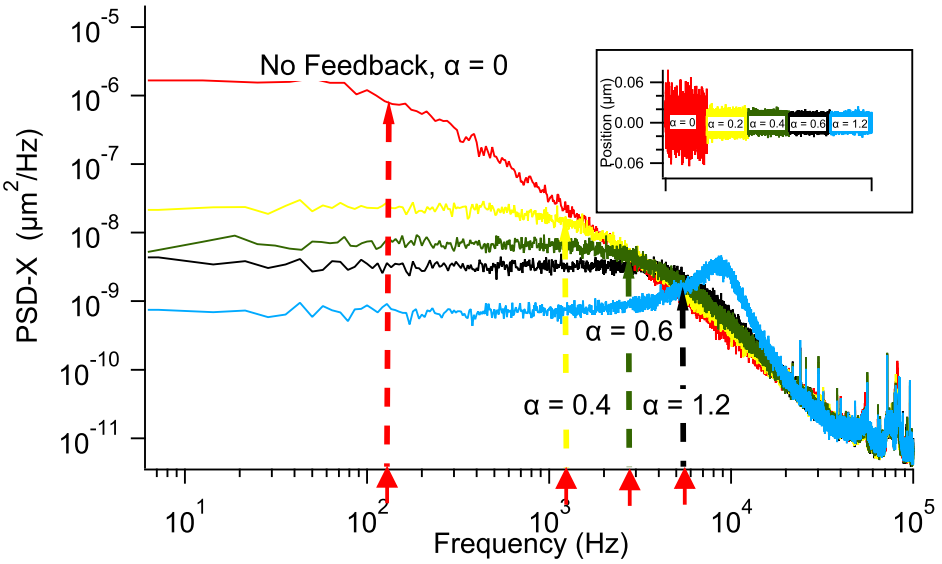

Figure 4. Power spectrum density of the x-signal from the QPD for different values of proportional feedback gains (α = 0, 0.4, 0.6, 1.2). As the feedback gain increases, the trap stiffness increases. The inset shows the time-series of particle position for different feedback gains. The variance decreases as the feedback gain increases.

5.2 Virtual double-well potential

One of the interesting applications of feedback traps is to create arbitrary time-dependent potentials. Here, we investigate a static virtual double-well potential. Such potentials have previously been created using single beam optical tweezers by rapidly scanning the trap centre between two positions.[26] These traps are limited in shapes. Multiplexed optical tweezers techniques fails when we need to change well separation and energy barriers separately. For our virtual potential, we parametrize a static double-well potential as

$$\frac{U(x)}{k_{\mathrm{B}}T} = 4\left(\frac{E_{\mathrm{b}}}{k_{\mathrm{B}}T}\right)\left[-\frac{1}{2}\left(\frac{x}{x_{\mathrm{m}}}\right)^2 + \frac{1}{4}\left(\frac{x}{x_{\mathrm{m}}}\right)^4\right] \tag{5.1}$$

where E_{b} is the potential barrier, x is particle's position scaled by the well position x_{m} and energy is scaled by $k_{\mathrm{B}}T$.

In Eq. (5.1), we see that we have independent control over well separation and energy barrier. To apply a double–well potential the force term in Eq. (3.2a) is replaced by $F = -\frac{\partial U(x,t)}{\partial x}$. Figure 5 shows the instantaneous hopping of a particle in a double–well potential with imposed barrier height $2k_{\mathrm{B}}T$ and the reconstructed potential from the time series. We see that the imposed potential (shown in blue in Fig. 5b) agrees well with the experimental result.

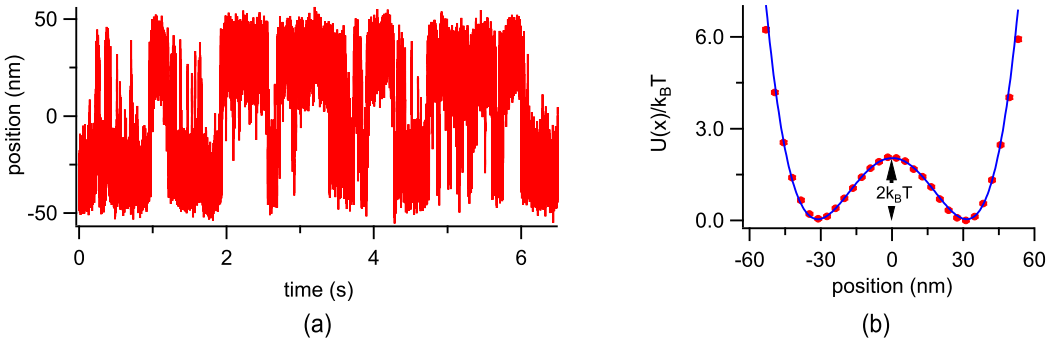

Figure 5. (a) Time series showing instantaneous hops over potential barrier. (b) Potential energy reconstructed from the particle's time trace using Boltzmann distribution. The imposed energy barrier, $E_{\rm b}/k_{\rm B}T$ is $2k_{\rm B}T$ and well separation, $x_{\rm m}$ is 30 nm.

We applied different barrier heights for our double-well (Fig. 6) keeping the well-separation fixed. The experimental results show a nice agreement with the theory. We expect theory to deviate from the experimental results for higher barriers.

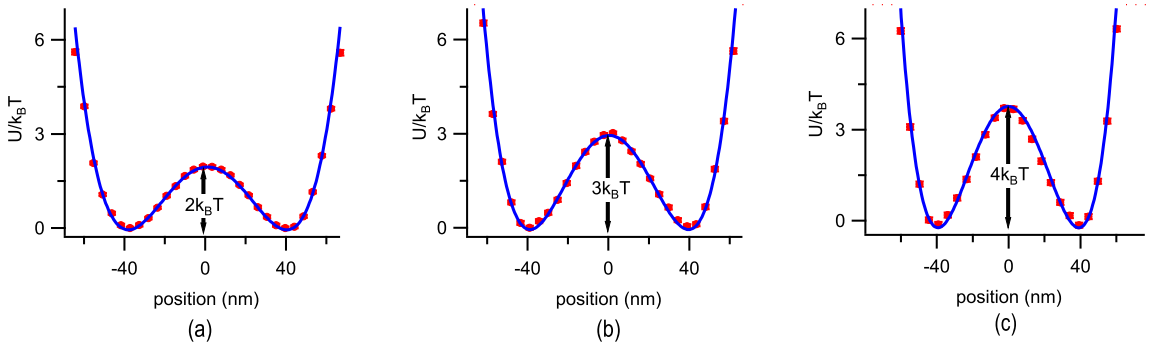

Figure 6. Virtual double-well potentials with different barrier heights. (a) $E_{\rm b} = 2k_{\rm B}T$, (b) $E_{\rm b} = 3k_{\rm B}T$ and (c) $E_{\rm b} = 4k_{\rm B}T$ and fixed well separation (39 nm). The plots shown in blue are imposed potentials for each case.

.

6. CONCLUSION

In this paper, we described our experimental setup to apply feedback forces using optical tweezers. We have shown that using feedback we can make the trap 35–40 stiffer than the actual underlying trap without increasing the laser power. This bandwidth is three times more than the results reported in Ref. 16. This technique will be useful for biological experiments where the trap strength is compromised by heating effect. Feedback traps can hold specimen firmly without damaging them.

We have also created a static double-well potential with tunable well-separation and the barrier height. Such control has not been demonstrated in time-shared traps. Feedback traps can be used to carry out stochastic thermodynamics experiments based on virtual potentials. We have used ABEL traps to impose slow protocols for memory-erasure experiments.[17] But real-world applications of thermodynamics are typically to finite-time transformations, and there are many open questions concerning the ultimate limits for such non-equilibrium situations. Our new feedback trap setup can impose faster protocols for such finite-time thermodynamic experiments.[27,28]

ACKNOWLEDGMENTS

The research work was supported by NSERC, Canada.

REFERENCES

[1] Ashkin, A., Dziedzic, J. M., Bjorkholm, J., and Chu, S., "Observation of a single-beam gradient force optical trap for dielectric particles," *Opt. Lett.* **11**, 288–290 (1986).

[2] Block, S. M., Goldstein, L. S., and Schnapp, B. J., "Bead movement by single kinesin molecules studied with optical tweezers," *Nature* **348**, 348 (1990).

[3] Woodside, M. T., Anthony, P. C., Behnke-Parks, W. M., Larizadeh, K., Herschlag, D., and Block, S. M., "Direct measurement of the full, sequence-dependent folding landscape of a nucleic acid," *Science* **314**, 1001–1004 (2006).

[4] Wang, M. D., Yin, H., Landick, R., Gelles, J., and Block, S. M., "Stretching DNA with optical tweezers," *Biophys. J.* **72**, 1335–1346 (1997).

[5] Mellor, C. D., Sharp, M. A., Bain, C. D., and Ward, A. D., "Probing interactions between colloidal particles with oscillating optical tweezers," *J. Appl. Phys.* **97**, 103114 (2005).

[6] Ashkin, A. and Dziedzic, J., "Feedback stabilization of optically levitated particles," *App. Phys. Lett.* **30**, 202–204 (1977).

[7] Gosse, C. and Croquette, V., "Magnetic tweezers: micromanipulation and force measurement at the molecular level," *Biophys. J.* **82**, 3314–3329 (2002).

[8] Armani, M. D., Chaudhary, S. V., Probst, R., and Shapiro, B., "Using feedback control of microflows to independently steer multiple particles," *J. Microelectromech S.* **15**, 945–956 (2006).

[9] Braun, M. and Cichos, F., "Optically controlled thermophoretic trapping of single nano-objects," *ACS Nano* **7**, 11200–11208 (2013).

[10] Lin, L., Wang, M., Peng, X., Lissek, E. N., Mao, Z., Scarabelli, L., Adkins, E., Coskun, S., Unalan, H. E., Korgel, B. A., et al., "Opto-thermoelectric nanotweezers.," *Nature Photonics* **12**, 195–201 (2018).

[11] Cohen, A. E., "Control of nanoparticles with arbitrary two-dimensional force fields," *Phys. Rev. Lett.* **94**, 118102 (2005).

[12] Cohen, A. E. and Moerner, W., "Method for trapping and manipulating nanoscale objects in solution," *App. Phys. Lett.* **86**, 093109 (2005).

[13] Jun, Y. and Bechhoefer, J., "Virtual potentials for feedback traps," *Phys. Rev. E* **86**, 061106 (2012).

[14] Simmons, R. M., Finer, J. T., Chu, S., and Spudich, J. A., "Quantitative measurements of force and displacement using an optical trap," *Biophys. J.* **70**, 1813–1822 (1996).

[15] Ranaweera, A. and Bamieh, B., "Modelling, identification, and control of a spherical particle trapped in an optical tweezer," *Int. J. Robust Nonlin.* **15**, 747–768 (2005).

[16] Wallin, A. E., Ojala, H., Hæggström, E., and Tuma, R., "Stiffer optical tweezers through real-time feedback control," *App. Phys. Lett.* **92**, 224104 (2008).

[17] Jun, Y., Gavrilov, M., and Bechhoefer, J., "High-precision test of landauer's principle in a feedback trap," *App. Phys. Lett.* **113**, 190601 (2014).

[18] Bérut, A., Arakelyan, A., Petrosyan, A., Ciliberto, S., Dillenschneider, R., and Lutz, E., "Experimental verification of Landauer's principle linking information and thermodynamics," *Nature* **483**, 187 (2012).

[19] Gavrilov, M., Jun, Y., and Bechhoefer, J., "Real-time calibration of a feedback trap," *Rev. Sci. Instrum.* **85**, 095102 (2014).

[20] Cohen, A. E., *Trapping and manipulating single molecules in solution*, PhD thesis, Stanford University (2007).

[21] Dufresne, E. R., Spalding, G. C., Dearing, M. T., Sheets, S. A., and Grier, D. G., "Computer-generated holographic optical tweezer arrays," *Rev Sci Instrum* **72**, 1810–1816 (2001).

[22] Brouhard, G. J., Schek, H. T., and Hunt, A. J., "Advanced optical tweezers for the study of cellular and molecular biomechanics," *IEEE Trans. Biomed. Eng* **50**, 121–125 (2003).

[23] Guilford, W. H., Tournas, J. A., Dascalu, D., and Watson, D. S., "Creating multiple time-shared laser traps with simultaneous displacement detection using digital signal processing hardware," *Anal. Biochem.* **326**, 153–166 (2004).

[24] Valentine, M. T., Guydosh, N. R., Gutiérrez-Medina, B., Fehr, A. N., Andreasson, J. O., and Block, S. M., "Precision steering of an optical trap by electro-optic deflection," *Opt. Lett.* **33**, 599–601 (2008).

[25] Hwang, S.-U., Park, I.-Y., Song, J.-H., Lee, Y.-G., LeBrun, T., Dagalakis, N., Gagnon, C., and Balijepalli, A., "Three-dimensional scanning optical tweezers," in [*Optomechatronic Actuators and Manipulation*], **6048**, 604803, International Society for Optics and Photonics (2005).

[26] Visscher, K., Brakenhoff, G., and Krol, J., "Micromanipulation by "multiple" optical traps created by a single fast scanning trap integrated with the bilateral confocal scanning laser microscope," *Cytometry A* **14**, 105–114 (1993).

[27] Aurell, E., Gawędzki, K., Mejía-Monasterio, C., Mohayaee, R., and Muratore-Ginanneschi, P., "Refined second law of thermodynamics for fast random processes," *J. Stat. Phys* **147**, 487–505 (2012).

[28] Zulkowski, P. R. and DeWeese, M. R., "Optimal finite-time erasure of a classical bit," *Phys. Rev. E* **89**, 052140 (2014).